arXiv:1411.1717v1 [cond-mat.supr-con] 6 Nov 2014

Enhancement of thermoelectric effect in diffusive superconducting bilayers with magnetic interfaces

Mikhail S. Kalenkov[1,2] and Andrei D. Zaikin[3,1]

[1] *I.E. Tamm Department of Theoretical Physics, P.N. Lebedev Physical Institute, 119991 Moscow, Russia*
[2] *Laboratory of Cryogenic Nanoelectronics, Nizhny Novgorod State Technical University, 603950 Nizhny Novgorod, Russia*
[3] *Institut für Nanotechnologie, Karlsruher Institut für Technologie (KIT), 76021 Karlsruhe, Germany*

We demonstrate that thermoelectric currents in superconducting bilayers with a spin-active interface are controlled by the two competing processes. On one hand, spin-sensitive quasiparticle scattering at such interface generates electron-hole imbalance and yields orders-of-magnitude enhancement of the thermoelectric effect in the system. On the other hand, this electron-hole imbalance gets suppressed in the superconductor bulk due to electron scattering on non-magnetic impurities. As a result, large thermoelectric currents can only flow in the vicinity of the spin-active interface and decay away from this interface at a distance exceeding the electron elastic mean free path ℓ. The magnitude of the thermoelectric effect reaches its maximum provided ℓ becomes of order of the total bilayer thickness.

PACS numbers: 74.25.fg, 74.45.+c, 74.78.Fk

I. INTRODUCTION

Thermoelectric effect in superconductors attracts a lot of attention over last decades[1]. Several earlier experiments[2–4] demonstrated that thermoelectric currents flowing in superconductors in the presence of a non-zero temperature gradient can reach values exceeding the standard theoretical predictions[5] by several orders of magnitude. While more experimental research is definitely needed to clarify the situation, on a theory side there has been a substantial progress allowing to pinpoint the basic physical reason that may yield a dramatic increase of the thermoelectric effect in superconducting compounds. It was argued by a number of authors that such an increase can be observed provided electron-hole symmetry is violated in the system. In this case thermoelectric currents do not anymore depend on a small parameter $T/\varepsilon_F \ll 1$ (where ε_F is the Fermi energy) and may reach values as high as the critical (depairing) current of a superconductor.

Theoretical models describing this physical situation are diverse embracing, e.g., conventional superconductors doped by magnetic impurities[6], unconventional superconductors with non-magnetic impurities[7], superconductor-ferromagnet hybrid structures with the density of states spin-split by the exchange and/or Zeeman fields[8,9] as well as various realizations of superconducting-normal (SN) hybrids[10–12] and superconducting bilayers[13]. In particular, one can consider an SN bilayer with a spin-active interface separating the two metals (see Fig. 1). Recently we demonstrated[12] that interface scattering rates for electrons and holes in such structures in general differ from each other thus providing a transparent physical mechanism for the electron-hole imbalance generation. The latter, in turn, results in huge thermoelectric currents flowing along the SN interface provided the left and the right ends of the bilayer are maintained at different temperatures.

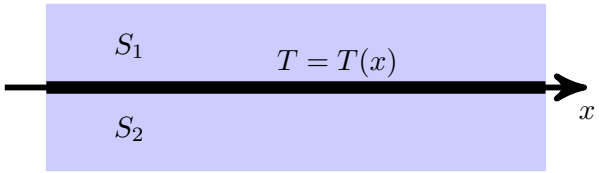

FIG. 1: A metallic bilayer which consists of two superconductors S_1 and S_2 separated by a spin-active interface. The temperature $T(x)$ changes only in the direction parallel to the interface.

For the sake of simplicity in[12,13] the limit of sufficiently clean metals was considered, in which case electrons and holes move ballistically and scatter only at the SN interface. In realistic metallic structures, however, quasiparticles may also scatter on non-magnetic impurities in the bulk of the sample, on various boundary imperfections and so on. As a result, quasiparticle motion inside a metal becomes diffusive rather than ballistic and the whole analysis[12,13] needs to be modified in order to account for a non-trivial interplay between non-magnetic impurity scattering and electron reflection at the spin-active SN interface. Investigation of the electron-hole imbalance and the thermoelectric effect under such conditions is the primary goal of our present work.

The structure of the paper is as follows. In section 2 we describe our quasiclassical formalism which is then employed in section 3 in order to quantitatively analyze the effect of electron scattering on non-magnetic impurities in our system. In section 4 we evaluate the thermoelectric current in disordered superconducting bilayers with spin-active intermetallic interfaces and present a brief discussion of our results. Some technical details of our calculation are displayed in Appendix.

II. QUASICLASSICAL FORMALISM

In what follows we will employ the quasiclassical theory of superconductivity. Within this theory the electric current density $\boldsymbol{j}$ in the system can be expressed in terms of the Keldysh component of the quasiclassical Green function

$$\boldsymbol{j}(\boldsymbol{r}) = -\frac{eN_0}{8}\int d\varepsilon \left\langle \boldsymbol{v}_F \,\mathrm{Sp}[\hat{\tau}_3 \hat{g}^K(\boldsymbol{p}_F, \boldsymbol{r}, \varepsilon)]\right\rangle, \quad (1)$$

where $\boldsymbol{p}_F = m\boldsymbol{v}_F$ is the electron Fermi momentum vector, $\hat{\tau}_3$ is the Pauli matrix in the Nambu space, N_0 is the normal density of states at the Fermi level, angular brackets $\langle\cdots\rangle$ denote averaging over the Fermi momentum directions and $\hat{g}^K$ is the Keldysh block of the full Green-Keldysh matrix

$$\check{g} = \begin{pmatrix} \hat{g}^R & \hat{g}^K \\ 0 & \hat{g}^A \end{pmatrix}, \quad (2)$$

Here and below the "check" symbol denotes the 8×8 matrices in the Keldysh⊗Nambu⊗Spin space whereas the "hat" symbol implies the 4×4 matrices in the Nambu⊗Spin space. The matrix function $\check{g}$ obeys the transport-like Eilenberger equations[14]

$$\left[\varepsilon\hat{\tau}_3 - \check{\Delta}(\boldsymbol{r}) - \check{\sigma}_{\mathrm{imp}}, \check{g}\right] + i\boldsymbol{v}_F\nabla\check{g}(\boldsymbol{p}_F, \boldsymbol{r}, \varepsilon) = 0 \quad (3)$$

together with the normalization condition

$$\check{g}^2 = 1. \quad (4)$$

Here the self-energy $\check{\sigma}_{\mathrm{imp}}$ accounts for elastic electron scattering off non-magnetic isotropic impurities randomly distributed in our sample. It has the standard form

$$\check{\sigma}_{\mathrm{imp}} = -i\frac{v_F}{2\ell}\langle\check{g}\rangle, \quad (5)$$

where ℓ is the electron elastic mean free path. The order parameter matrix $\check{\Delta}$ contains non-vanishing retarded and advanced components

$$\hat{\Delta}^A = \hat{\Delta}^R = \begin{pmatrix} 0 & \Delta\sigma_0 \\ -\Delta^*\sigma_0 & 0 \end{pmatrix}, \quad \hat{\Delta}^K = 0, \quad (6)$$

where σ_0 is the unity matrix in the spin space and Δ is the superconducting order parameter which will be chosen real throughout our consideration.

The above quasiclassical equations should be supplemented by the proper boundary conditions matching Green functions for incoming and outgoing momentum directions on both sides of the interface (see Fig. 2). Similarly to our earlier works[12,13], here we will also assume that the two metals forming a bilayer are separated by a spin-active interface provided, e.g., by a thin ferromagnetic layer. The corresponding boundary conditions for the quasiclassical propagators at such interfaces were formulated in Ref.[15]. Below we will use an equivalent approach developed in Ref.[16].

We will stick to a simple model describing spin-dependent electron scattering at the interface. This model involves three parameters, i.e. the two interface transmission probabilities $D_\uparrow$ and $D_\downarrow$ describing opposite spin directions as well as the so-called spin mixing angle θ which is just the difference between the scattering phase shifts for the spin-up and spin-down electrons. Within this model the elements of the interface S-matrix take the form

$$S_{11} = S_{22} = \sqrt{R_\sigma}e^{i\theta_\sigma/2}, \quad (7)$$

$$S_{12} = S_{21} = i\sqrt{D_\sigma}e^{i\theta_\sigma/2}, \quad (8)$$

$$\underline{S}_{11} = \underline{S}_{22} = \sqrt{R_{-\sigma}}e^{-i\theta_\sigma/2}, \quad (9)$$

$$\underline{S}_{12} = \underline{S}_{21} = i\sqrt{D_{-\sigma}}e^{-i\theta_\sigma/2}, \quad (10)$$

where $\theta_\sigma = \theta\sigma_3$ is the 2×2 diagonal matrix in the spin space. The matrices $R_{\pm\sigma}$, $D_{\pm\sigma}$ are defined as

$$R_\sigma = \begin{pmatrix} R_\uparrow & 0 \\ 0 & R_\downarrow \end{pmatrix}, \quad R_{-\sigma} = \begin{pmatrix} R_\downarrow & 0 \\ 0 & R_\uparrow \end{pmatrix}, \quad (11)$$

$$D_\sigma = \begin{pmatrix} D_\uparrow & 0 \\ 0 & D_\downarrow \end{pmatrix}, \quad D_{-\sigma} = \begin{pmatrix} D_\downarrow & 0 \\ 0 & D_\uparrow \end{pmatrix}, \quad (12)$$

where $R_\uparrow = 1 - D_\uparrow$ and $R_\downarrow = 1 - D_\downarrow$ are the electron reflection probabilities for the corresponding spin direction. The above matrices constitute the building blocks of the full S-matrix for electrons

$$\mathcal{S} = \begin{pmatrix} S_{11} & S_{12} \\ S_{21} & S_{22} \end{pmatrix}, \quad (13)$$

and holes

$$\underline{\mathcal{S}} = \begin{pmatrix} \underline{S}_{11} & \underline{S}_{12} \\ \underline{S}_{21} & \underline{S}_{22} \end{pmatrix}. \quad (14)$$

In what follows it will be convenient for us to make use of the so-called Riccati parameterization[17,18] for the Green functions involving four Riccati amplitudes and two distribution functions (see appendix A for more details). Following[18] we denote the distribution functions x and the Riccati amplitudes γ by the upper-case and the lower-case letters depending on the quasiparticle Fermi momentum (see Fig. 2):

$$\check{g}_{i,\mathrm{in}} = \check{g}_{i,\mathrm{in}}[\gamma_i^R, \tilde{\Gamma}_i^R, \Gamma_i^A, \tilde{\gamma}_i^A, x_i, \tilde{X}_i], \quad i = 1,2, \quad (15)$$

$$\check{g}_{i,\mathrm{out}} = \check{g}_{i,\mathrm{out}}[\Gamma_i^R, \tilde{\gamma}_i^R, \gamma_i^A, \tilde{\Gamma}_i^A, X_i, \tilde{x}_i], \quad i = 1,2, \quad (16)$$

where the Riccati amplitudes γ, $\tilde{\gamma}_i$, Γ_i, $\tilde{\Gamma}_i$ and the distribution functions x_i, $\tilde{x}_i$, X_i, $\tilde{X}_i$ are all 2×2 matrices in the spin space. The boundary conditions at the spin-active interface[16] express the interface values of the "upper-case" functions Γ and X in terms of the "lower-case" ones γ and x.

III. EFFECT OF IMPURITY SCATTERING

Let us now investigate the effect of impurity scattering in superconducting bilayers consisting of two superconductors S_1 and S_2 situated respectively in half-spaces

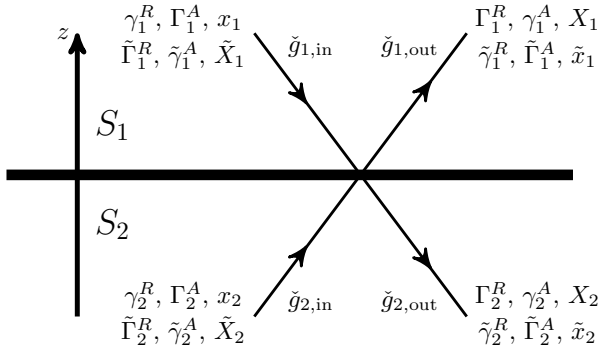

FIG. 2: Boundary conditions matching the Green functions for incoming and outgoing momentum directions on both sides of the interface.

$z>0$ and $z<0$ and separated by a spin-active interface. All quantities will be labeled by the index 1 or 2 depending on whether they belong to the first or the second superconductor.

We will assume that the temperature $T=T(x)$ varies slowly as a function of the coordinate x along the interface and does not depend on the coordinates y and z. Then the Keldysh Green function can be written in the form

$$\hat g_i^K = \left[\hat g_i^R - \hat g_i^A\right]\tanh\frac{\varepsilon}{2T(x)} + \hat g_i^a, \tag{17}$$

where the term $\hat g_i^a$ is proportional to the temperature gradient $\partial_x T$ and, hence, remains sufficiently small. The Green function $\hat g_i^a$ for incoming and outgoing momentum directions can be parameterized by the two distribution functions

$$\hat g^a_{i,in} = 2\frac{\begin{pmatrix} x_i^a - \gamma_i^R\tilde X_i^a\tilde\gamma_i^A & x_i^a\Gamma_i^A - \gamma_i^R\tilde X_i^a \\ \tilde X_i^a\tilde\gamma_i^A - \tilde\Gamma_i^R x_i^a & \tilde X_i^a - \tilde\Gamma_i^R x_i^a\Gamma_i^A\end{pmatrix}}{\left[1-\gamma_i^R\tilde\Gamma_i^R\right]\left[1-\tilde\gamma_i^A\Gamma_i^A\right]}, \tag{18}$$

$$\hat g^a_{i,out} = 2\frac{\begin{pmatrix} X_i^a - \Gamma_i^R\tilde x_i^a\tilde\Gamma_i^A & X_i^a\gamma_i^A - \Gamma_i^R\tilde x_i^a \\ \tilde x_i^a\tilde\Gamma_i^A - \tilde\gamma_i^R X_i^a & \tilde x_i^a - \tilde\gamma_i^R X_i^a\gamma_i^A\end{pmatrix}}{\left[1-\gamma_i^R\tilde\Gamma_i^R\right]\left[1-\tilde\gamma_i^A\Gamma_i^A\right]}. \tag{19}$$

Here we already made use of the fact that within our model all matrices are diagonal in the spin space. The functions x_i^a, $\tilde x_i^a$, X_i^a, $\tilde X_i^a$ are non-equilibrium parts of the distribution functions, i.e.

$$x_i = (1-\gamma_i^R\tilde\gamma_i^A)\tanh\frac{\varepsilon}{2T(x)} + x_i^a, \tag{20}$$

$$\tilde x_i = -(1-\tilde\gamma_i^R\gamma_i^A)\tanh\frac{\varepsilon}{2T(x)} + \tilde x_i^a, \tag{21}$$

$$X_i = (1-\Gamma_i^R\tilde\Gamma_i^A)\tanh\frac{\varepsilon}{2T(x)} + X_i^a, \tag{22}$$

$$\tilde X_i = -(1-\tilde\Gamma_i^R\Gamma_i^A)\tanh\frac{\varepsilon}{2T(x)} + \tilde X_i^a. \tag{23}$$

As our final goal is to evaluate the thermoelectric current flowing along the interface between two superconductors, it is instructive to obtain the expression for the corresponding combination which enters into Eq. (1), i.e.

$$\mathrm{Sp}(\hat\tau_3\hat g^a_{i,\rm in} + \hat\tau_3\hat g^a_{i,\rm out}) = 2\,\mathrm{Sp}\left[\frac{(X_i^a-\tilde X_i^a)(1+\gamma_i^R\gamma_i^A)}{(1-\gamma_i^R\Gamma_i^R)(1-\gamma_i^A\Gamma_i^A)}\right]. \tag{24}$$

Here we already employed the condition $x_i^a=\tilde x_i^a$ satisfied within the linear response approximation we are going to use. The combination (24) contains a small factor $X_i^a - \tilde X_i^a$ proportional to the temperature gradient $\partial_x T$. This observation enables us to evaluate the Riccati amplitudes in Eq. (24) in thermodynamic equilibrium.

With the aid of the boundary conditions one can establish the relations between the interface values of the Riccati amplitudes. They read

$$\Gamma_1^R(0) = \left[\gamma_1^R(0)\sqrt{R_\uparrow R_\downarrow} + \gamma_2^R(0)\sqrt{D_\uparrow D_\downarrow} - \right.$$
$$\left. - \gamma_1^R(0)(\gamma_2^R(0))^2 e^{i\theta_\sigma}\right]\left[1-(\gamma_2^R(0))^2\sqrt{R_\uparrow R_\downarrow}e^{i\theta_\sigma} - \right.$$
$$\left. - \gamma_2^R(0)\gamma_1^R(0)\sqrt{D_\uparrow D_\downarrow}e^{i\theta_\sigma}\right]^{-1} e^{i\theta_\sigma}, \tag{25}$$

$$\Gamma_1^A(0) = \left[\gamma_1^A(0)\sqrt{R_\uparrow R_\downarrow} + \gamma_2^A(0)\sqrt{D_\uparrow D_\downarrow} - \right.$$
$$\left. - \gamma_1^A(0)(\gamma_2^A(0))^2 e^{-i\theta_\sigma}\right]\left[1-(\gamma_2^A(0))^2\sqrt{R_\uparrow R_\downarrow}e^{-i\theta_\sigma} - \right.$$
$$\left. - \gamma_2^A(0)\gamma_1^A(0)\sqrt{D_\uparrow D_\downarrow}e^{-i\theta_\sigma}\right]^{-1} e^{-i\theta_\sigma}. \tag{26}$$

The analogous expressions for $\Gamma_2^{R,A}(0)$ are derived from the above equations by means of a trivial index replacement $1\leftrightarrow 2$. In the equilibrium Riccati amplitudes depend on energy ε, momentum $\boldsymbol{p}_F$ and coordinate z. Note that for brevity we do not indicate explicitly the dependence of Riccati amplitudes on the energy ε and momentum $\boldsymbol{p}_F$ arguments. We also note that the equations for the tilde Riccati amplitudes are redundant because of the identities $\tilde\gamma_i^{R,A}=\gamma_i^{R,A}$ and $\tilde\Gamma_i^{R,A}=\Gamma_i^{R,A}$ which remain applicable as long as the superconducting order parameter is chosen real.

With the aid of the above quasiclassical equations it is straightforward to demonstrate that the difference $X_i^a - \tilde X_i^a$ obeys the equation

$$i|v_z|(\mathrm{sgn}\,z)\partial_z(X_i^a-\tilde X_i^a) +$$
$$+\left(\tilde\varepsilon_i^R - \tilde\varepsilon_i^A - \tilde\Delta_i^R\Gamma_i^R + \tilde\Delta_i^A\Gamma_i^A\right)(X_i^a-\tilde X_i^a) = 0, \tag{27}$$

where $\tilde\varepsilon_i^{R,A}$ and $\tilde\Delta_i^{R,A}$ are respectively the renormalized energy and the order parameter defined as

$$\begin{pmatrix}\tilde\varepsilon_i^{R,A} & \tilde\Delta_i^{R,A} \\ -\tilde\Delta_i^{R,A} & -\tilde\varepsilon_i^{R,A}\end{pmatrix} = \begin{pmatrix}\varepsilon & \Delta_i \\ -\Delta_i & -\varepsilon\end{pmatrix} - \hat\sigma^{R,A}_{i,\rm imp}. \tag{28}$$

Eq. (27) can easily be resolved with the result

$$X_i^a(z) - \tilde X_i^a(z) = \frac{[1-\gamma_i^R(z)\Gamma_i^R(z)][1-\gamma_i^A(z)\Gamma_i^A(z)]}{[1-\gamma_i^R(0)\Gamma_i^R(0)][1-\gamma_i^A(0)\Gamma_i^A(0)]}\times$$
$$\times\left[X_i^a(0)-\tilde X_i^a(0)\right]\exp\left(-\frac{2\,\mathrm{sgn}\,z}{|v_z|}\int_0^z w_i(z')dz'\right), \tag{29}$$

where

$$2iw_i = \tilde{\varepsilon}_i^R - \tilde{\varepsilon}_i^A - \tilde{\Delta}_i^R\gamma_i^R + \tilde{\Delta}_i^A\gamma_i^A, \tag{30}$$

Exploiting the boundary conditions we can express the difference $X_i^a(0) - \tilde{X}_i^a(0)$ at the interface in terms of the interface values $x_i^a(0)$,

$$X_1^a(0) - \tilde{X}_1^a(0) = (R_\uparrow - R_\downarrow)\left[1 - \gamma_2^R(0)\gamma_2^A(0)\right]\sigma_3 \times \\ \times \frac{\left[1 + \gamma_2^R(0)\gamma_2^A(0)\right]x_1^a(0) - \left[1 + \gamma_1^R(0)\gamma_1^A(0)\right]x_2^a(0)}{\left|1 - (\gamma_2^R(0))^2\sqrt{R_\uparrow R_\downarrow}e^{i\theta_\sigma} - \gamma_2^R(0)\gamma_1^R(0)\sqrt{D_\uparrow D_\downarrow}e^{i\theta_\sigma}\right|^2}, \tag{31}$$

and similarly for $X_2^a(0) - \tilde{X}_2^a(0)$.

The interface value $x_i^a(0)$ is recovered from the equation

$$2|v_z|\,\mathrm{sgn}\, z\partial_z x_i^a + w_i x_i^a = -v_x\frac{\varepsilon(1 - \gamma_i^R\gamma_i^A)}{T^2\cosh^2(\varepsilon/2T)}\partial_x T, \tag{32}$$

which yields

$$x_1^a(0) = \frac{v_x\varepsilon\partial_x T}{2|v_z|T^2\cosh^2(\varepsilon/2T)} \times \\ \times \int_0^\infty \left[1 - \gamma_1^R(z)\gamma_1^A(z)\right]\exp\left(-\frac{2}{|v_z|}\int_0^z w_1(z')dz'\right)dz. \tag{33}$$

An analogous expression can be established for $x_2^a(0)$.

Introducing the characteristic lengths $L_i^\pm$ defined by means of the equations

$$\int_0^\infty [1 \pm \gamma_1^R(z)\gamma_1^A(z)]\exp\left(-\frac{2}{|v_z|}\int_0^z w_1(z')dz'\right)dz = \\ = \frac{|v_z|}{v_F}[1 \pm \gamma_1^R(0)\gamma_1^A(0)]L_1^\pm, \tag{34}$$

and

$$\int_{-\infty}^0 [1 \pm \gamma_2^R(z)\gamma_2^A(z)]\exp\left(-\frac{2}{|v_z|}\int_z^0 w_2(z')dz'\right)dz = \\ = \frac{|v_z|}{v_F}[1 \pm \gamma_2^R(0)\gamma_2^A(0)]L_2^\pm, \tag{35}$$

one can conveniently rewrite the interface values $x_i^a(0)$ in a compact form

$$x_i^a(0) = \frac{v_x\left[1 - \gamma_i^R(0)\gamma_i^A(0)\right]\varepsilon L_i^-}{2v_F T^2\cosh^2(\varepsilon/2T)}\partial_x T. \tag{36}$$

The above equations allow to fully describe the effect of electron scattering on non-magnetic impurities and to evaluate the thermoelectric currents in the system under consideration.

IV. THERMOELECTRIC CURRENTS

Combining the results derived in the previous section, from Eq. (1) we obtain the expression for the current density, e.g., in the superconductor S_1 ($z > 0$). It reads

$$j_1(z) = -\frac{eN_0}{8v_F}\partial_x T\int\frac{\varepsilon d\varepsilon}{T^2\cosh^2(\varepsilon/2T)}\Big\langle v_x^2\Theta(-v_z)\times \\ \times (R_\uparrow - R_\downarrow)\,\mathrm{Sp}\Big\{\sigma_3\mathcal{A}_1^+(z)\exp\left(-\frac{2}{|v_z|}\int_0^z w_1(z')dz'\right)\times \\ \times \mathcal{A}_2^-(0)\left[\mathcal{A}_2^+(0)\mathcal{A}_1^-(0)L_1^- - \mathcal{A}_1^+(0)\mathcal{A}_2^-(0)L_2^-\right]\mathcal{N}\Big\}\Big\rangle, \tag{37}$$

where

$$\mathcal{N} = \big|1 - (\gamma_1^R(0))^2\sqrt{R_\uparrow R_\downarrow}e^{i\theta_\sigma} - (\gamma_2^R(0))^2\sqrt{R_\uparrow R_\downarrow}e^{i\theta_\sigma} - \\ - 2\gamma_2^R(0)\gamma_1^R(0)\sqrt{D_\uparrow D_\downarrow}e^{i\theta_\sigma} + (\gamma_2^R(0)\gamma_1^R(0))^2e^{2i\theta_\sigma}\big|^{-2}, \tag{38}$$

$$\mathcal{A}_i^\pm(z) = 1 \pm \gamma_i^R(z)\gamma_i^A(z), \tag{39}$$

and $\Theta(y)$ is the Heavyside step function. The current density in the superconductor S_2 ($z < 0$) is obtained from Eq. (37) by replacing $1 \leftrightarrow 2$ and $\int_0^z \leftrightarrow \int_z^0$. From these results we observe that thermoelectric currents on two sides of the interface have opposite signs, i.e. these currents can flow in *opposite directions*.

It also follows from the above results that impurity scattering leads to the exponential decay of the current density far from the spin-active interface. The characteristic length of the decay is controlled by function w_i and depends both on the electron energy and on its momentum direction. Far from the interface the function w_i can easily be established analytically since in this limit the retarded and advanced Green functions tend to their bulk values. After a simple calculation one finds

$$w_i(\varepsilon) = \begin{cases} \dfrac{v_F}{2\ell_i}, & |\varepsilon| > \Delta_i, \\ \dfrac{v_F}{2\ell_i} + \sqrt{\Delta_i^2 - \varepsilon^2}, & |\varepsilon| < \Delta_i, \end{cases} \tag{40}$$

This result implies that the thermoelectric current is confined to the interface and decays deep into the superconducting bulk at a typical length not exceeding the corresponding elastic mean free path $\ell_{1(2)}$.

Integrating Eq. (37) over z we obtain the net thermoelectric current flowing along the interface

$$I = -\frac{eN_0}{8v_F^2}\partial_x T\int\frac{\varepsilon d\varepsilon}{T^2\cosh^2(\varepsilon/2T)}\Big\langle v_{f,x}^2|v_z|\Theta(-v_z)\times \\ \times (R_\uparrow - R_\downarrow)\,\mathrm{Sp}\Big\{\sigma_3\left[\mathcal{A}_2^-(0)\mathcal{A}_1^+(0)L_1^+ - \mathcal{A}_1^-(0)\mathcal{A}_2^+(0)L_2^+\right]\times \\ \times \left[\mathcal{A}_2^+(0)\mathcal{A}_1^-(0)L_1^- - \mathcal{A}_1^+(0)\mathcal{A}_2^-(0)L_2^-\right]\mathcal{N}\Big\}\Big\rangle. \tag{41}$$

Just as in the ballistic limit, the above expression for the thermoelectric current becomes zero if the interface transmission probabilities for the opposite spin directions coincide $D_\uparrow = D_\downarrow$ and/or the spin mixing angle θ equals to zero. In addition, the current density (37) and, hence, also the total current (41) vanish for identical superconductors S_1 and S_2 (in this case one has $\gamma_1^{R(A)}(0) = \gamma_2^{R(A)}(0)$ and $L_1^\pm = L_2^\pm$) indicating the absence of the electron-hole asymmetry in this specific limit.

Provided $D_\uparrow \neq D_\downarrow$, $\theta \neq 0$ and the superconductors S_1 and S_2 are not identical (one of them can also be a normal metal) the current (41) does not vanish and under certain conditions can reach values orders of magnitude higher than, e.g., in normal metals. The exact evaluation of Eq. (41) in a general case can only be performed numerically. However, simple estimates can be obtained in certain limits.

For instance, in the tunneling limit $D_\uparrow, D_\downarrow \ll 1$ and for the case of diffusive superconductors with very different mean free path values (i.e. for $\ell_1^2 + \ell_2^2 \gg \ell_1\ell_2$) the expression (41) reduces to a much simpler form:

$$I = \frac{eN_0}{8v_F^2}\partial_x T \int \frac{(\ell_1^2+\ell_2^2)\varepsilon d\varepsilon}{T^2\cosh^2(\varepsilon/2T)}\Big\langle v_x^2|v_z|\Theta(-v_z)\times \\ \times (D_\uparrow - D_\downarrow)\left[\nu_{1\uparrow}(0)\nu_{2\uparrow}(0) - \nu_{1\downarrow}(0)\nu_{2\downarrow}(0)\right]\Big\rangle, \quad (42)$$

where $\nu_{i\uparrow(\downarrow)}(0)$ are the momentum and energy resolved densities of states at the interface for the opposite electron spin orientations.

At intermediate temperatures $T \sim \Delta$ we can roughly estimate the magnitude of the thermoelectric current as

$$I \sim eN_0 v_F \ell^2 (R_\uparrow - R_\downarrow)\sin\theta \partial_x T. \quad (43)$$

It is instructive to compare this result with the thermoelectric current $I_{\rm norm}$ flowing in our bilayer in its normal state. Making use of the well known Mott relation for the thermoelectric coefficient of normal metals, from (43) we obtain

$$\frac{I}{I_{\rm norm}} \sim \frac{\ell}{d}\frac{\varepsilon_F}{T_c}(R_\uparrow - R_\downarrow)\sin\theta, \quad (44)$$

where d is the total thickness of our bilayer, T_c is the critical temperature of the bulk superconductor. Setting $\ell \sim d$, $R_\uparrow - R_\downarrow \sim 1$ and $\sin\theta \sim 1$ we immediately arrive at the conclusion that the thermoelectric current I in the superconducting state can be enhanced by a very large factor up to $\varepsilon_F/T_c \gg 1$ as compared to that in the normal state $I_{\rm norm}$.

Summarizing our results, we arrive at the following physical picture. Different scattering rates for electrons and holes at the spin-active interface result in electron-hole imbalance generation[12] which in turn may yield to orders-of-magnitude enhancement of thermoelectric currents in our system. On the other hand, scattering on non-magnetic impurities tends to suppress this imbalance deep in the metal bulk. Hence, large thermoelectric currents can only flow in the vicinity of the interface. The characteristic current decay length L_i^+ away from the interface turns out to be of order of the corresponding elastic mean free path. E.g., in the diffusive limit (i.e. provided ℓ_i remains shorter than the superconducting coherence length) one simply has $L_i^+ = L_i^- = \ell_i$. Accordingly, the magnitude of the thermoelectric current I increases with increasing ℓ_i and reaches its maximum when the elastic mean free becomes of order of the total bilayer thickness d, cf. Eq. (44). A similar trend was also observed within a different model of a superconductor doped by magnetic impurities[6].

Let us also note that although the general structure of Eq. (37) is quite similar to that of our earlier results[12,13] derived for ballistic bilayers, it is not possible to directly recover the latter by setting $\ell_i \to \infty$ in the expression (37). This is because our present results were derived under the assumption about the existence of a local temperature $T(x)$ in our system slowly varying along the x-axis. Accordingly, Eq. (37) holds under the condition $\ell_i \lesssim T/|\partial_x T|$. No such condition was employed in the analysis[12,13].

Nevertheless, a formal replacement $L_i^- \partial_x T \to \Delta T$ (where ΔT is the total temperature difference applied to our system) together with putting ℓ_i equal to infinity makes the structure of Eq. (37) fully equivalent to that of the ballistic result[12,13]. The latter observation implies that our main conclusion about the parametric enhancement of the thermoelectric effect in superconducting structures with spin-active interfaces is robust and is not sensitive to the details of the adopted model.

MSK acknowledges support from Grant NNSTU No. 11.G34.31.0029 under Russian Governement Decree #220.

Appendix A: Green function parameterization

In the course of our analysis we employ the so-called Riccati parameterization[17,18] for the retarded and advanced Green functions, i.e. we set

$$\hat{g}^{R,A} = \pm\hat{N}^{R,A}\begin{pmatrix} 1+\gamma^{R,A}\tilde{\gamma}^{R,A} & 2\gamma^{R,A} \\ -2\tilde{\gamma}^{R,A} & -1-\tilde{\gamma}^{R,A}\gamma^{R,A}\end{pmatrix}, \quad (A1)$$

where

$$\hat{N}^{R,A} = \begin{pmatrix} (1-\gamma^{R,A}\tilde{\gamma}^{R,A})^{-1} & 0 \\ 0 & (1-\tilde{\gamma}^{R,A}\gamma^{R,A})^{-1}\end{pmatrix}. \quad (A2)$$

and the Riccati amplitudes $\gamma^{R,A}$, $\tilde{\gamma}^{R,A}$ are 2×2 matrices in the spin space. The expression for the Keldysh Green function contains two distribution functions x^K, $\tilde{x}^K$ also being 2×2 matrices in spin space

$$\hat{g}^K = 2\hat{N}^R\begin{pmatrix} x^K - \gamma^R\tilde{x}^K\tilde{\gamma}^A & -\gamma^R\tilde{x}^K + x^K\gamma^A \\ -\tilde{\gamma}^R x^K + \tilde{x}^K\tilde{\gamma}^A & \tilde{x}^K - \tilde{\gamma}^R x^K\gamma^A\end{pmatrix}\hat{N}^A. \quad (A3)$$

The amplitudes $\gamma^{R,A}$, $\tilde{\gamma}^{R,A}$ obey the Riccati equation

$$i\boldsymbol{v}_F\nabla\gamma^{R,A} = \begin{pmatrix}1 & \gamma^{R,A}\end{pmatrix}\hat{h}^{R,A}\begin{pmatrix}-\gamma^{R,A}\\ 1\end{pmatrix}, \tag{A4}$$

$$i\boldsymbol{v}_F\nabla\tilde{\gamma}^{R,A} = \begin{pmatrix}\tilde{\gamma}^{R,A} & 1\end{pmatrix}\hat{h}^{R,A}\begin{pmatrix}1\\ -\tilde{\gamma}^{R,A}\end{pmatrix}, \tag{A5}$$

and the distribution functions x^K and $\tilde{x}^K$ satisfy the transport-like equations

$$i\boldsymbol{v}_F\nabla x^K = x^K\begin{pmatrix}1 & 0\end{pmatrix}\hat{h}^A\begin{pmatrix}1\\ -\tilde{\gamma}^A\end{pmatrix} + \\ + \begin{pmatrix}1 & \gamma^R\end{pmatrix}\hat{h}^K\begin{pmatrix}1\\ -\tilde{\gamma}^A\end{pmatrix} - \begin{pmatrix}1 & \gamma^R\end{pmatrix}\hat{h}^R\begin{pmatrix}1\\ 0\end{pmatrix}x^K, \tag{A6}$$

and

$$i\boldsymbol{v}_F\nabla\tilde{x}^K = \tilde{x}^K\begin{pmatrix}0 & 1\end{pmatrix}\hat{h}^A\begin{pmatrix}-\gamma^A\\ 1\end{pmatrix} - \\ - \begin{pmatrix}\tilde{\gamma}^R & 1\end{pmatrix}\hat{h}^K\begin{pmatrix}-\gamma^A\\ 1\end{pmatrix} - \begin{pmatrix}\tilde{\gamma}^R & 1\end{pmatrix}\hat{h}^R\begin{pmatrix}0\\ 1\end{pmatrix}\tilde{x}^K. \tag{A7}$$

Here the matrices $\hat{h}^{R,A,K}$ denote respectively the retarded, advanced and Keldysh components of the matrix $\check{h} = \varepsilon\hat{\tau}_3 - \check{\Delta}(\boldsymbol{r}) - \check{\sigma}_{\rm imp}$.

[1] V.L. Ginzburg, Rev. Mod. Phys. **76**, 981 (2004).
[2] N.V. Zavaritskii, JETP Lett. **19**, 126 (1974).
[3] C.M. Falco, Solid St. Commun. **19**, 623 (1976).
[4] D.J. Van Harlingen, D.F. Heidel, and J.C. Garland, Phys. Rev. B **21**, 1842 (1980).
[5] Yu.M. Gal'perin, V.L. Gurevich, and V.I. Kozub, JETP Lett. **17**, 476 (1973).
[6] M.S. Kalenkov, A.D. Zaikin, and L.S. Kuzmin, Phys. Rev. Lett. **109**, 147004 (2012).
[7] T. Löfwander and M. Fogelström, Phys. Rev. B **70**, 024515 (2004).
[8] P. Machon, M. Eschrig, and W. Belzig, Phys. Rev. Lett. **110**, 047002 (2013); New J. Phys. **16**, 073002 (2014).
[9] A. Ozaeta, P. Virtanen, F.S. Bergeret, and T.T. Heikkilä, Phys. Rev. Lett. **112**, 057001 (2014).
[10] R. Seviour and A.F. Volkov, Phys. Rev. B **62**, R6116 (2000).
[11] A.F. Volkov and V.V. Pavlovskii, Phys. Rev. B **72**, 014529 (2005).
[12] M.S. Kalenkov and A.D. Zaikin, Phys. Rev. B **90**, 134502 (2014).
[13] M.S. Kalenkov and A.D. Zaikin, arXiv:1410.4021 (unpublished).
[14] W. Belzig, F. Wilhelm, C. Bruder, G. Schön, and A.D. Zaikin, Superlatt. Microstruct. **25**, 1251 (1999).
[15] A. Millis, D. Rainer, and J.A. Sauls, Phys. Rev. B **38** 4504 (1988).
[16] E. Zhao, T. Löfwander, and J.A. Sauls, Phys. Rev. B **70** 134510 (2004).
[17] N. Schopohl and K. Maki, Phys. Rev. B **52**, 490 (1995); N. Schopohl, cond-mat/9804064 (unpublished).
[18] M. Eschrig, Phys. Rev. B **61**, 9061 (2000).